



AFRL-RZ-WP-TP-2009-2249

EFFECTS OF REACTING CROSS-STREAM FLOW ON TURBINE FILM COOLING (Postprint)

**Wesly S. Anderson, Marc D. Polanka, Joseph Zelina, Dave S. Evans, Scott D. Stouffer, and
Garth R. Justinger**

**Combustion Branch
Turbine Engine Division**

JANUARY 2010

Approved for public release; distribution unlimited.

See additional restrictions described on inside pages

STINFO COPY

©2008 ASME

**AIR FORCE RESEARCH LABORATORY
PROPULSION DIRECTORATE
WRIGHT-PATTERSON AIR FORCE BASE, OH 45433-7251
AIR FORCE MATERIEL COMMAND
UNITED STATES AIR FORCE**

REPORT DOCUMENTATION PAGE					<i>Form Approved</i> OMB No. 0704-0188	
The public reporting burden for this collection of information is estimated to average 1 hour per response, including the time for reviewing instructions, searching existing data sources, gathering and maintaining the data needed, and completing and reviewing the collection of information. Send comments regarding this burden estimate or any other aspect of this collection of information, including suggestions for reducing this burden, to Department of Defense, Washington Headquarters Services, Directorate for Information Operations and Reports (0704-0188), 1215 Jefferson Davis Highway, Suite 1204, Arlington, VA 22202-4302. Respondents should be aware that notwithstanding any other provision of law, no person shall be subject to any penalty for failing to comply with a collection of information if it does not display a currently valid OMB control number. PLEASE DO NOT RETURN YOUR FORM TO THE ABOVE ADDRESS.						
1. REPORT DATE (DD-MM-YY) January 2010		2. REPORT TYPE Conference Proceedings Postprint		3. DATES COVERED (From - To) 01 October 2007 – 01 October 2009		
4. TITLE AND SUBTITLE EFFECTS OF REACTING CROSS-STREAM FLOW ON TURBINE FILM COOLING (Postprint)				5a. CONTRACT NUMBER IN HOUSE		
				5b. GRANT NUMBER		
				5c. PROGRAM ELEMENT NUMBER 62203F		
6. AUTHOR(S) Wesly S. Anderson, Marc D. Polanka, and Joseph Zelina (AFRL/RZTC) Dave S. Evans (Naval Air Systems Command) Scott D. Stouffer and Garth R. Justinger (University of Dayton Research Institute)				5d. PROJECT NUMBER 3048		
				5e. TASK NUMBER 04		
				5f. WORK UNIT NUMBER 304804CC		
7. PERFORMING ORGANIZATION NAME(S) AND ADDRESS(ES) <div style="display: flex; justify-content: space-between;"> <div style="width: 45%;"> Combustion Branch (AFRL/RZTC) Turbine Engine Division Air Force Research Laboratory, Propulsion Directorate Wright-Patterson Air Force Base, OH 45433-7251 Air Force Materiel Command, United States Air Force </div> <div style="width: 45%;"> Naval Air Systems Command NAS Patuxent River, MD ----- University of Dayton Research Institute Dayton, OH </div> </div>				8. PERFORMING ORGANIZATION REPORT NUMBER AFRL-RZ-WP-TP-2009-2249		
9. SPONSORING/MONITORING AGENCY NAME(S) AND ADDRESS(ES) Air Force Research Laboratory Propulsion Directorate Wright-Patterson Air Force Base, OH 45433-7251 Air Force Materiel Command United States Air Force				10. SPONSORING/MONITORING AGENCY ACRONYM(S) AFRL/RZTC		
				11. SPONSORING/MONITORING AGENCY REPORT NUMBER(S) AFRL-RZ-WP-TP-2009-2249		
12. DISTRIBUTION/AVAILABILITY STATEMENT Approved for public release; distribution unlimited.						
13. SUPPLEMENTARY NOTES PA case number 88ABW-2008-0003; cleared 24 November 2008. ©2008 ASME. This work was funded in whole or in part by Department of the Air Force Work Unit Number 304804CC. The U.S. Government has for itself and others acting on its behalf a paid-up, nonexclusive, irrevocable worldwide license to use, modify, reproduce, release, perform, display, or disclose the work by or on behalf of the U. S. Government. Paper contains color.						
14. ABSTRACT Film cooling plays a critical role in providing effective thermal protection to components in modern gas turbine engines. A significant effort has been undertaken over the last 40 years to improve the distribution of coolant and to ensure that the airfoil is protected by this coolant from the hot gases in the freestream. This film, under conditions with high fuel air ratios, may actually be detrimental to the underlying metal. The presence of unburned fuel from an upstream combustor may interact with this oxygen rich film coolant jet resulting in secondary combustion. The completion of the reactions can increase the gas temperature locally resulting in higher heat transfer to the airfoil directly along the path line of the film coolant jet. This secondary combustion could damage the turbine blade, resulting in costly repair, reduction in turbine life, or even engine failure. However, knowledge of film cooling in a reactive flow is very limited. The current study explores the interaction of cooling flow from typical cooling holes with the exhaust of a fuel-rich well-stirred reactor operating at high temperatures over a flat plate.						
15. SUBJECT TERMS High-g Combustion, Ultra-Compact Combustor, Inter-Turbine Burner, film-cooling, heat transfer						
16. SECURITY CLASSIFICATION OF:			17. LIMITATION OF ABSTRACT: SAR	18. NUMBER OF PAGES 16	19a. NAME OF RESPONSIBLE PERSON (Monitor) CAPT Wesly S. Anderson, USAF 19b. TELEPHONE NUMBER (Include Area Code) (937) 255-6814	
a. REPORT Unclassified	b. ABSTRACT Unclassified	c. THIS PAGE Unclassified				

GT2009-59242

EFFECTS OF A REACTING CROSS-STREAM ON TURBINE FILM COOLING

Wesly S. Anderson

Marc D. Polanka

Joseph Zelina

Air Force Research Lab, Propulsion Directorate

Wright Patterson AFB, Dayton, OH, USA

Dave S. Evans

Naval Air Systems Command

NAS Patuxent River, MD

Scott D. Stouffer

Garth R. Justinger

University of Dayton Research Institute

Dayton, OH, USA

ABSTRACT

Film cooling plays a critical role in providing effective thermal protection to components in modern gas turbine engines. A significant effort has been undertaken over the last 40 years to improve the distribution of coolant and to ensure that the airfoil is protected by this coolant from the hot gases in the freestream. This film, under conditions with high fuel air ratios, may actually be detrimental to the underlying metal. The presence of unburned fuel from an upstream combustor may interact with this oxygen rich film coolant jet resulting in secondary combustion. The completion of the reactions can increase the gas temperature locally resulting in higher heat transfer to the airfoil directly along the path line of the film coolant jet. This secondary combustion could damage the turbine blade, resulting in costly repair, reduction in turbine life, or even engine failure. However, knowledge of film cooling in a reactive flow is very limited. The current study explores the interaction of cooling flow from typical cooling holes with the exhaust of a fuel-rich well-stirred reactor operating at high temperatures over a flat plate. Surface temperatures, heat flux, and heat transfer coefficients are calculated for a variety of reactor fuel-to-air ratios, cooling hole geometries, and blowing ratios. Emphasis is placed on the difference between a normal cylindrical hole, an inclined cylindrical hole, and a fan shaped cooling hole. When both air and nitrogen are injected through the cooling holes, the changes in surface temperature can be directly correlated to the presence of the reaction. Photographs of the localized burning are presented to verify the extent and locations of the reaction.

NOMENCLATURE

A	=	area (m ²)
D	=	diameter (m)
Da	=	Damkohler number
h	=	heat transfer coefficient (W/m ² ·K)
M	=	blowing ratio
\dot{m}	=	mass flow rate (g/min; g/s)
q''	=	heat flux (W/m ²)
T	=	temperature (K)
U	=	velocity (m/s)
x	=	location; distance (m)
Φ	=	equivalence ratio
ρ	=	density (kg/m ³)

Subscripts

∞	=	freestream; reactor exhaust stream
c	=	coolant; convection
eff	=	effective
f	=	film
s	=	surface

INTRODUCTION

Film cooling is the primary means of maintaining turbine surface temperatures below the critical melting temperature. The most common cooling hole configurations are normal cylindrical holes, angled cylindrical holes, and fan shaped holes. Countless studies have been conducted over the past forty years that have investigated the merits of different cooling schemes under nearly all conditions encountered in a turbine. A review article by Bogard and Thole [1] addresses many of the relevant issues. The impact of the inclination angle was studied by Baldauf et al. [2] revealing that at low blowing ratios the angled holes exhibit better performance because the coolant flow remains attached to the surface over a longer

distance. At the higher blowing ratios, the relative differences between normal and angled holes diminish and the normal holes can be more effective. The relative benefits of cylindrical, fan shaped, and laidback fan shaped holes have also been studied by Saumweber et al [3]. The laidback fan shaped hole ejects more coolant flow at a lower blowing ratio. Because of the increasing area of the hole near the exit, this configuration also reduces the tendency of the jet to separate. These benefits associated with shaping are dramatic, particularly at high blowing ratios, resulting in higher effectiveness.

One area that has not been investigated thoroughly is the impact of combustion gases on the film cooling process. Historically, the combustion sections of gas turbine engines have operated at overall equivalence ratios (Φ) much less than one [4]. Additionally, a relatively long flow path within the combustor (on the order of 25-50 cm) compared to chemical and mixing times ensured that reactions were complete before leaving the combustor. Therefore, no unburned species enter the turbine and subsequently little concern has been expressed in the literature. Recently, however, the desire to increase performance has led to the development of combustors that operate at an Φ much closer to one. With these designs, the chance of fuel rich streaks entering the turbine increases. At the same time, advanced combustors are being designed more compact to increase the thrust to weight ratios. One such design is the Ultra-Compact Combustor/Inter-Turbine Burner (UCC/ITB) currently being developed at the Air Force Research Laboratories (AFRL) [5-6]. Figure 1 contains images of a conventional annular combustor (left) and the UCC (right). This concept directs the flow of combustion air into a circumferential cavity for providing sufficient residence times while at the same time reducing the axial length of the component. Fuel is injected into this cavity, where combustion occurs in a fuel rich regimes. The flow is then entrained into a radial cavity that is integrated with the vane. Because of the close proximity, the gases in this cavity still contain intermediate combustion products.

The possibility of unburned fuel entering the turbine,

therefore, can no longer be ignored. The primary location where the fuel can find an oxygen rich stream to complete the reaction is at the film cooling hole. The chances of reactions occurring in the turbine vastly increase. When the unburned fuel mixes with oxygen rich compressor bleed air in the turbine cooling film, conditions become conducive for burning in the turbine. Heat release in the cooling film, whether it results from recombination of dissociated species or from the combustion of unburned fuel, would drastically reduce the cooling effectiveness of the turbine cooling scheme, with potentially severe effects on engine component durability. The challenges presented by this design require a fuller understanding of the interaction between turbine cooling films and incomplete combustion products as well as the relationship between boundary layer reactions and turbine durability.

The potential effect of heat release in the turbine was studied by Lukachko et al. [7] who found that the potential local temperature rise depends strongly on the amount of chemical energy remaining in the flow. The research showed that the local temperature increase in a flow simulating a fuel streak in a future combustor at a stoichiometric fuel to air ratio could become large and potentially catastrophic. In a subsequent effort by Kirk et al. [8], a series of shock tube experiments were conducted that examined the impact of near wall reactions in a cooling film. Their experimental setup allowed concurrent heat flux measurements for a reacting (air) coolant flow and a nonreacting (N_2) coolant flow through a 35° injection angle into a freestream mixture of ethylene and argon. Blowing ratios in the test ranged from 0.5 to 2.0, for a range of unburned fuel concentrations. Their research showed that at high concentrations of unburned fuel, as much as a 30% increase in heat flux may occur. At moderate CO concentrations, the increase reaches approximately 10%. At low concentrations, the difference between reacting and nonreacting flows is insignificant. The objective of the present research is to explore the effect of reactions on turbine film cooling. Specifically, the impact of blowing ratio, equivalence ratio, and cooling hole shape on the occurrence of heat release on a flat plate geometry are quantified. A Well Stirred Reactor (WSR) was employed to

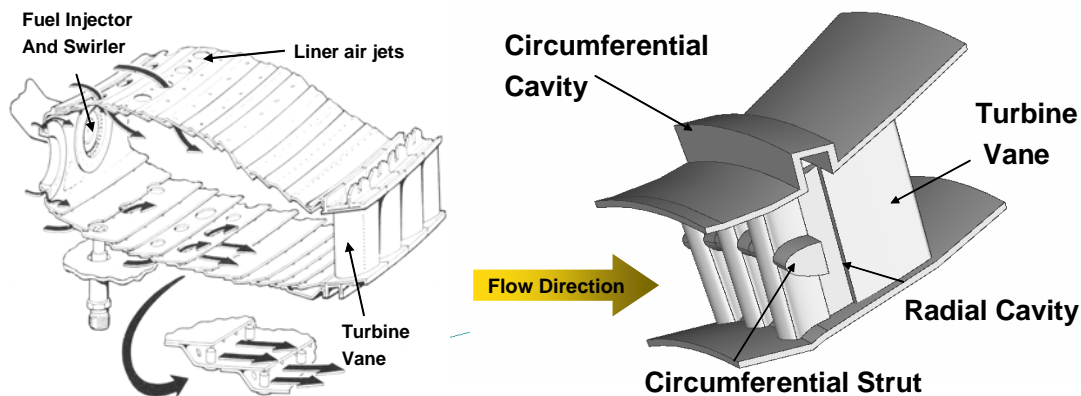


Figure 1. Conventional axial combustor (left) and Ultra-Compact combustor (right) [5]

provide a well characterized source of combustion products utilizing propane as a fuel source. Propane was chosen as it has a similar heat release as liquid jet fuel while being more chemically accurate to the molecular weight of the species expected to be present within the turbine section. This research will serve as an incremental step toward understanding the physics of reacting boundary layers as they relate to compact combustion systems such as the UCC, where the turbine vane is integrated into the combustor design. The ultimate goal of this program is to provide a sufficient understanding for the development of turbine cooling schemes that will enable the application of the UCC/ITB to future systems.

EXPERIMENTAL SETUP

A WSR, as developed by Nenniger et al. [9] and modified by Zelina [10] and Stouffer et al. [11], was used to simulate the turbine entry conditions of a notional combustor. In a WSR, a high rate of mixing of products and incoming reactants is induced which results in a very nearly uniform distribution of temperature and species within the reactor and at the exit. Because of the uniformity of the flow at the exit, it is possible to assume a uniform species and temperature distribution at a given distance within the test section. The mass flow rate and Φ into the reactor were controlled by thermal mass flow controllers.

The reactor is composed primarily of two toroidal half sections of cast zirconia-oxide ceramic, an Inconel[®] jet ring, and a metal housing. A schematic of the WSR is shown in Figure 2. Premixed air and fuel is fed through the fuel-air tubes into the jet ring, into the jet ring manifold, and through 48 fuel air jets into the reactor toroid. The two toroidal half sections fit together on the top and bottom of the jet ring, forming a 250 ml internal volume. Once in the reactor, the fuel-air mixture reacts and then exits through eight exhaust ports. The flow then enters a common exhaust section, which turns the flow upwards into the test section. A temperature limit of 1970 K restricted the use of the reactor at equivalence ratios close to one at the high overall air flow rates that were desired to match the inlet Reynolds number. A gas sample was fed from the WSR to a standard emissions test bench for characterization of gas concentrations. CO₂ and CO were measured with a California Analytical Instruments FTIR analyzer. O₂ was measured with a Horiba magnetopneumatic analyzer.

From the WSR the exhaust flowed upwards through a shaped ceramic chimney, over a forward facing step that served as a turbulent trip, and into the test section. The test section consisted of a thick flat plate base that was enclosed by three quartz window side walls. Slots were machined in the piece to allow for the insertion of two cooling air assemblies and four heat transfer gauge assemblies. Each of these assemblies was inserted through the back of plate, with their surfaces flush with the surface of the plate.

The cooling air assemblies were made up of the cooling hole slot inserts and the plena. Cooling air or nitrogen was fed to the plena from the facility supply. In the plena, the cooling air temperature and pressure were measured. The plena were

attached to the cooling hole inserts and sealed with a high temperature adhesive sealant. Thermocouples were inserted to a location 5.1 mm from the outside surface of the cooling hole inserts. The cooling air assemblies were inserted through the back of the flat plate. The cooling hole geometries were machined into the surface of the inserts. Three film cooling configurations were tested as part of this study: normal holes, angled holes, and fan-shaped laidback holes (Figure 3). All the holes were 0.51 mm diameter. The normal holes had a length to diameter ratio (L/D) of 5. The spacing between the holes was 3.81 mm.

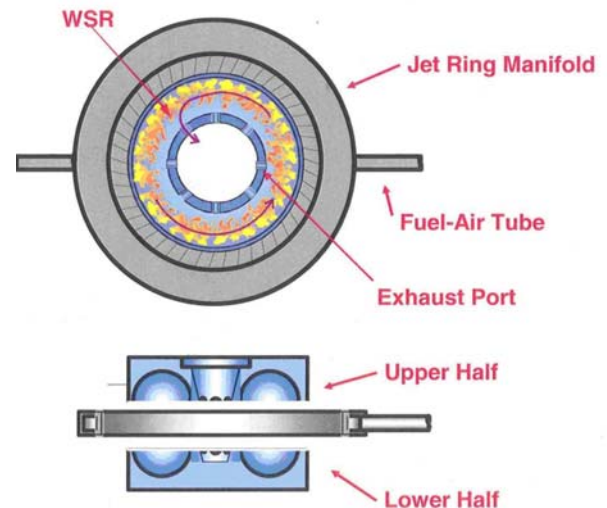


Figure 2. WSR schematic, modified from Stouffer [12]

The angled holes were machined at an angle of 30° to the surface. To maintain an L/D of 5, the surface was thinner. The fan-shaped laidback holes were based on the angled hole geometry, being equal in size, angle, and depth. However, at the surface that sees the flow, the sides of the hole flare out 10° and lay back 10° as well providing an exit hole length of 0.91 mm on the surface.

In the current study the heat transfer to the surface is utilized to determine the amount of heat release in the film. The heat transfer is calculated from measurements of two thermocouples embedded in instrumentation blocks downstream of the film cooling holes. The upper gauge was located 3.8 mm from the surface of the block. A second thermocouple was inserted through the bottom of the block to a depth of 19.1 mm from the surface. This provided a known distance between these thermocouples (15.3 mm). The conductivity of the Hastelloy-X[®] was determined locally by utilizing a linearization of the conductivity of Hastelloy-X[®] as a function of temperature from the manufacturer's material property data sheets. With these parameters being known, the heat flux can be determined directly from Fourier's Law. Steady, one dimensional conduction was confirmed by analyzing a typical set of boundary conditions with an ANSYS thermal conduction solver. Within the instrumentation blocks the temperature was determined to be nearly one dimensional.

Based on this result, the surface temperature was extrapolated using the embedded measurements and the calculated heat transfer. Four instrumentation blocks were installed, two at nominally 20 hole diameters downstream of the film coolant hole and the other two at approximately 75 diameters downstream. The surface of the flat plate with all inserts installed is shown in Figure 4. Also shown in this figure is the location of the film cooling row of 11 holes and the location of a second, upstream, film cooling port that was intended to simulate an upstream coolant row that will be used in future tests. Not shown in this figure is a trip strip that was installed at the leading edge (bottom of the picture) of the plate to ensure a turbulent boundary layer at the film cooling hole location.

One necessary addition to the test section was water channels to maintain the entire film cooled surface below the melting temperature of the material. A simple heat balance calculation indicated that the Hastelloy-X would achieve a surface temperature of 1600 K without active cooling. Because of the uncooled leading edge section and the desire to run at low coolant flow rates, it was necessary to water cool this surface. As shown in Figure 4, a five pass water circuit was included. To maintain a one dimensional temperature profile in the area of interest, the wall thickness was 5.1 cm and the circuits were 6.4 mm in diameter and installed about 13 mm from the bottom of the flat plate. The impact of the water circuit was investigated by Evans et al [13]. The water circuit controlled the temperatures between 850K on the hot surface and 450K at the deep thermocouple location.

For a comparison with the current literature it was beneficial to calculate the heat transfer coefficient in the presence of film cooling h_f . The traditional means of determining h_f in a film cooling layer would be with the use of Equation (1) where T_f is the driving temperature for the heat transfer and is the temperature of the film located adjacent to the surface and T_s is the temperature of the surface.

$$q'' = h_f(T_f - T_s) \quad (1)$$

It is a goal of this program to be able to experimentally measure T_f locally above the surface with the use of laser diagnostics, but at the current time T_f has not been measured. Therefore, Eq. (1) is modified with T_∞ as the reference temperature, and h_f is replaced with the effective heat transfer coefficient, h_{eff} . This effective heat transfer coefficient will therefore take into account changes locally of the film temperature due to heat release as this cannot currently be separated. Equation (2) is the form of the convective heat transfer equation used in the analysis of the results of this study.

$$q'' = h_{eff}(T_\infty - T_s) \quad (2)$$

Many fluid mechanical factors influence the film cooling behavior. The current study explores a number of these in addition to the chemistry of the flow: blowing ratio, injection angle, and hole shape. The blowing ratio, M , also referred to as the mass flux ratio, is given in Equation (3) as a ratio of densities and velocities.

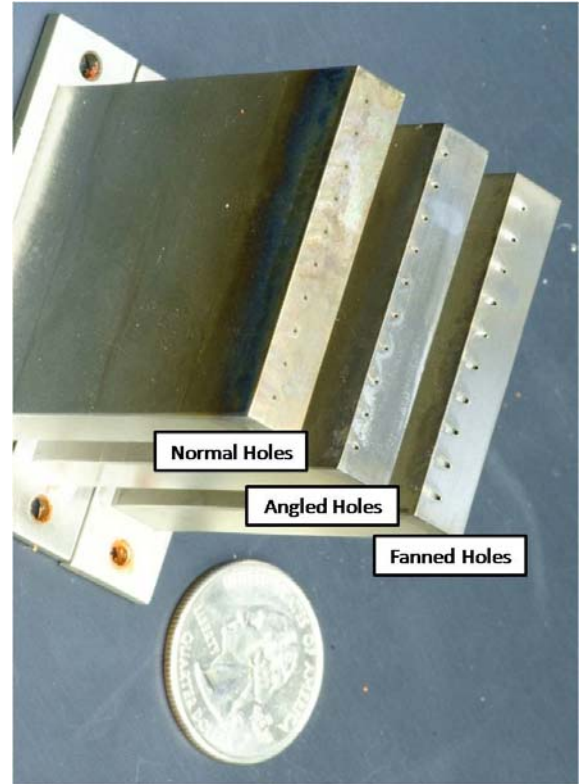


Figure 3. Cooling insert geometries

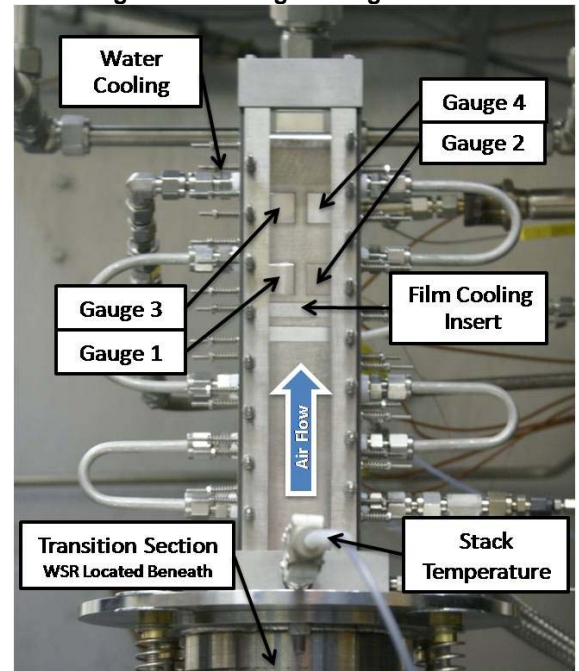


Figure 4. Flat plate heat transfer gauge and cooling hole insert location

$$M = \frac{\rho_c U_c}{\rho_\infty U_\infty} \quad (3)$$

The calculation of M directly from Eq. (3) requires precise knowledge of the density of the gases. The determination of this property in reacting systems is imprecise. Therefore, M was calculated in this experiment using the conservation of mass for a constant area flow in an incompressible fluid for both coolant flow and reactor exhaust flow. This yields the following:

$$M = \frac{\dot{m}_{c,total} A_{\infty}}{\dot{m}_{\infty} A_{c,total}} \quad (4)$$

Here, $\dot{m}_{c,total}$ is the total mass flow of the coolant through all cooling holes, $A_{c,total}$ is the metered area of all cooling holes, A_{∞} is the cross-sectional area of the test rig, and \dot{m}_{∞} is the mass flow of the reactor exhaust, equaling the sum of \dot{m}_{fuel} and \dot{m}_{air} .

The ratio of \dot{m}_{fuel} to \dot{m}_{air} is the fuel air ratio. This ratio compared to the value at the stoichiometric condition is the equivalence ratio. This ratio is given as:

$$\Phi = \frac{\left(\frac{\dot{m}_{fuel}}{\dot{m}_{air}}\right)}{\left(\frac{\dot{m}_{fuel}}{\dot{m}_{air}}\right)_{stoich}} \quad (5)$$

where the stoichiometric value of the fuel air ratio is 0.06395, for propane. With this definition, a Φ greater than one would be fuel rich and conversely, a Φ less than one would be fuel lean. More details of the measurements and calculations can be found in Evans et al. [13].

RESULTS

An extensive test matrix was built to understand the impact of heat release on a film cooled surface. This matrix focused on investigating the three typical film cooling hole arrangements shown in Figure 3. For each of these test plates, a series of experiments was performed with both nitrogen as the film coolant and then with air ejecting from the holes. A sequence of blowing ratios was established covering $M = 0, 0.5, 1.0, 1.5$, and 2.0 . Each test configuration was performed at equivalence ratios of $0.6, 0.8, 1.5, 1.6$, and 1.7 at a relatively

high air flow of 1020 g/min . This set the freestream velocity to be 34 m/s which correlated to a freestream Reynolds number of about $60,000$ based on the channel height or 600 based on the hole diameter. Equivalence ratios closer to 1.0 could not be achieved at this air flow rate because of the resultant WSR and stack exit temperature being too high. The materials used in the reactor were not capable of withstanding these higher temperatures. Therefore a few cases were performed at equivalence ratio of 0.8 and 0.95 at lower air flows of 720 and 480 g/min . These lower air flows were also repeated at the $\Phi = 1.5$ condition to permit comparison. A previous effort, Evans et al. [13], provides the impact of main airflow on the results.

In performing these tests a prominent white flame was evident just downstream of the coolant holes for the higher equivalence ratios. The flame was not present for any condition of Φ less than 1.0 . While readily visible to the naked eye, it was somewhat challenging to capture digitally mainly because of the viewing angle and the amount of light saturating the camera. The photographs were taken from the side of the rig, with the field of view restricted to the area immediately around the cooling holes. One good set of images was captured in Figure 5 for the angled hole case, at a $\Phi = 1.5$, showing the differences between the blowing ratio of $0, 0.5, 1.0$, and 1.5 for the air flow and the stark contrast at $M = 1.0$ for the nitrogen coolant flow. As the coolant jet met and mixed with the reactor exhaust flow, local combustion occurred. The combustion is visible as a white plume emanating from the coolant hole and progressing downstream.

These photographs demonstrate that boundary layer reactions can occur in fuel rich conditions as a result of the introduction of air from cooling holes. The reactions happen in close proximity to the surface and cause significant heat transfer to the surface in the immediate vicinity of the cooling holes. This visual evidence is proof of the cause for the heat transfer augmentation that will follow and is discerning to the turbine cooling designer. Instead of the film cooling flow serving to maintain the airfoil surface below a specific temperature, this oxygen rich flow is serving as a flame holder for any remaining combustion products to reach completion. As shown for this fuel rich condition, as the blowing ratio is

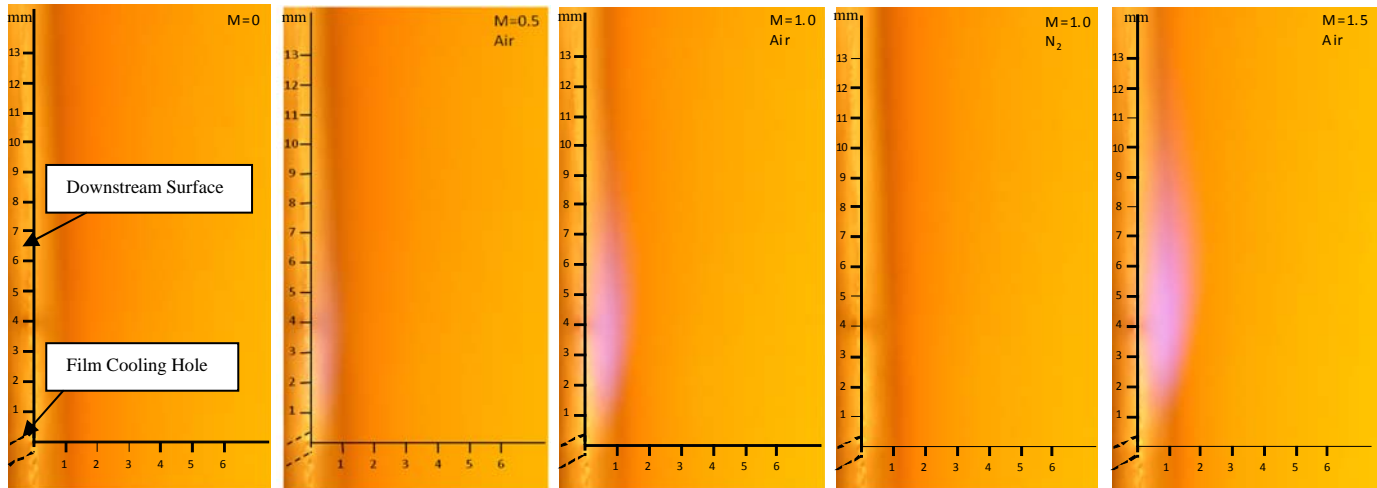


Figure 5. Angled hole visible burning for a) $M=0$ b) $M=0.5$, air c) $M=1.0$, air d) $M=1.0$, N_2 e) $M=1.5$, air

increased, the amount of burning is also increased. One small benefit is that for these angled holes at the higher blowing ratio, the jet itself is lifted off the surface. Therefore the highest temperatures are achieved away from the airfoil surface.

While the photographs of the visible flame provide qualitative proof of what was occurring in the flowfield, the measurements of temperature within the block and the subsequent reduction to heat flux provided the quantitative impact of that flame. The primary comparison made was a relative comparison between the air coolant flow and the nitrogen coolant flow. These two conditions were always obtained on the same day of testing for each configuration and the order was often alternated as the blowing ratio was varied to ensure that the trends were consistent. Also a given blowing ratio was occasionally repeated later in the test program to verify that the facility was not changing throughout the testing window. This was done for a number of reasons, the most significant was that the two set of blocks on either side of the rig often produced results with a substantial side to side variation. That is while the changes between gauges one and three were consistent with the changes between gauges two and four within approximately 5K, gauge 1 could be higher or lower than block 2 by 20K or more for a given test day or period within a test. It was thought that some residual variation within the well stirred reactor occurred because of some localized plugging of some of the feed holes that caused different flow to the different areas of the rig. Over the course of a test window, the characteristics of this distribution could change. Laser diagnostics are planned to further quantify these localized variations in the inlet condition.

What was ultimately verified was that the side to side trend in the blocks held true throughout when the results for air were compared to those for nitrogen. An uncertainty of about 1% was measured in surface temperature and subsequent heat flux between repeat points within a test period. A greater variation of closer to 5% occurred in an individual surface temperature with about a 4% change in the resultant heat flux when trying to reestablish the same condition on a different day. This was often due to changes in the WSR exit stack temperature and or the coolant exit temperature which were both difficult to

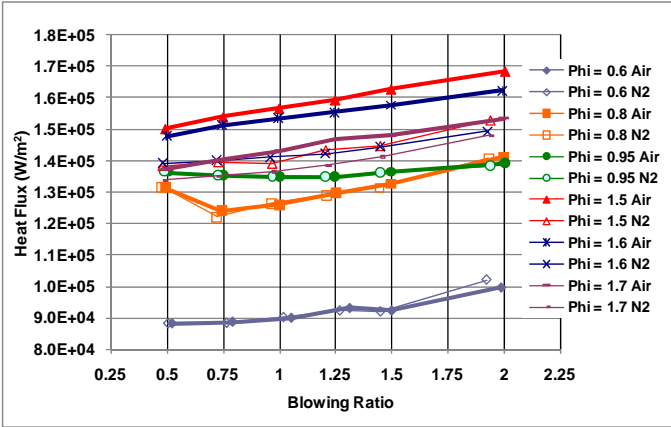


Figure 6. Angled Hole Heat Flux as a Function of Equivalence Ratio and Coolant Gas at $x/D = 20$

control day to day. However the difference between the air results and the nitrogen results was consistent, with variation within 2%. To account for some of the overall variation, the results presented in the following figures are mean values of measurements for gauges 1 and 2 for the 20 D location and between gauges 3 and 4 for the 75 D location.

The heat flux for the three cooling hole arrangements at an $x/D = 20$ is provided in Figures 6-8. In Figure 6 the angled hole results are shown for Φ of 0.6, 0.8, 0.95, 1.5, 1.6, and 1.7. It is noted that the $\Phi = 0.95$ data were obtained at a lower overall airflow of 720 g/min. Two primary results were realized. First, the overall heat flux levels differ at the different equivalence ratios, which is mostly due to the difference in the freestream temperature as Φ was changed. There was some variability between test days for this value but Table 1 provides the nominal variation in stack temperature with equivalence ratio. Again, this is the temperature achieved at the lower overall airflow for the $\Phi = 0.95$ case. This variation was absorbed by utilization of the effective heat transfer coefficient to be discussed in detail later. The second result was the marked difference in heat flux between the air and nitrogen coolant gases at the same Φ and blowing ratio for the equivalence ratios greater than 1.0. This is attributed to the local heat addition due to the reaction chemistry shown in Figure 5. It is likely that the reactions were initiated by auto-ignition as the inlet temperatures run in the experiment were well above those necessary for auto-ignition in hydrocarbon fuels. It is also possible that the flame contained in the WSR propagated into the test section causing ignition.

Table 1. Comparison of Stack Temperatures at Different Equivalence Ratios

Equivalence Ratio	0.6	0.8	0.95	1.5	1.6	1.7
Stack Temperature (K)	1525	1777	1827	1845	1805	1760

A similar result is depicted in Figure 7 for the normal hole case. Here, the heat flux at each equivalence ratio for nitrogen is somewhat higher than that found for the angled holes, which

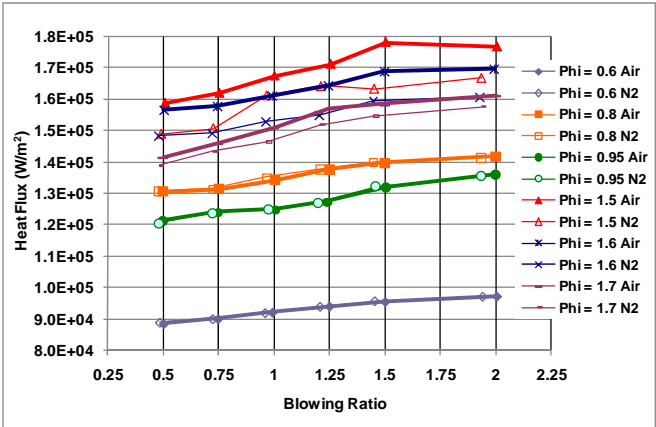


Figure 7. Normal Hole Heat Flux as a Function of Equivalence Ratio and Coolant Gas at $x/D = 20$

is consistent with the literature (Baldauf et al. [2] for example). What is different is that the heat flux augmentation was substantially higher for the angled holes than for the normal holes when the equivalence ratio was over 1.0. This can be directly attributed to the poorer film cooling coverage of the normal holes. Since, particularly at higher blowing ratios, the normal holes separate from the airfoil surface, the reaction is occurring off the surface, thus transferring less additional heat to the wall. Laser diagnostic measurements are planned in later experiments to try to determine exactly where the reactions are taking place for all three test conditions.

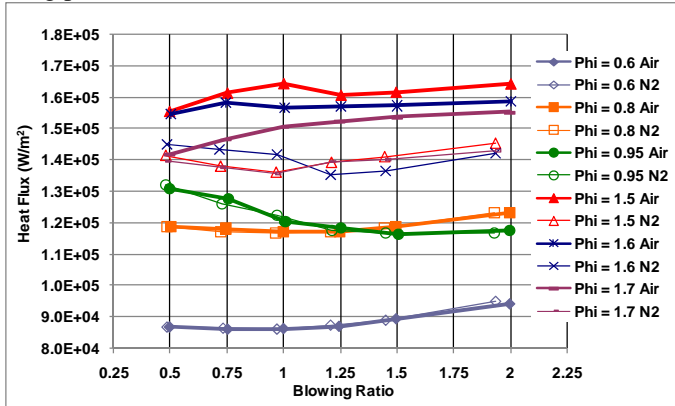


Figure 8. Fan Shaped Hole Heat Flux as a Function of Equivalence Ratio and Coolant Gas at $x/D = 20$

A contrary result is revealed in Figure 8 for the heat flux for the shaped hole configuration. Here, the heat flux values are lower than those for the angled hole configuration because of the more effective spread of coolant as is often observed in the literature (Saumweber et al. [3] as example). But as clearly seen in Figure 8, when the equivalence ratio was over 1.0, the augmentation experienced by the air fed cooling condition is the greatest of any case because the coolant flow was maintained very close to the surface. Attached flow is traditionally desirable for an effective cooling arrangement. However, in this case, having air close to the wall caused the heat release due to reaction to also be maintained near the wall. This resulted in a marked increase in the heat transfer.

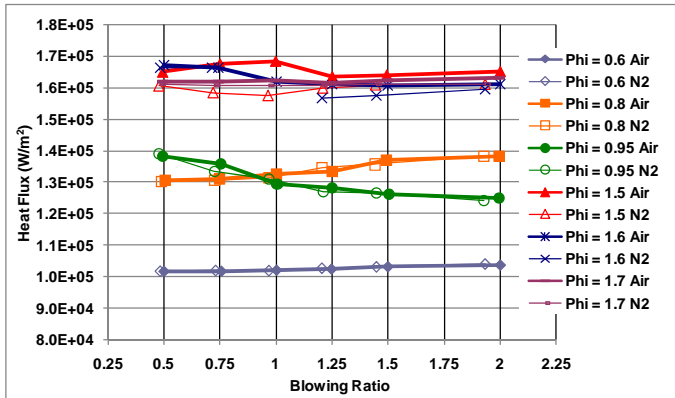


Figure 9. Fan Shaped Hole Heat Flux as a Function of Equivalence Ratio and Coolant Gas at $X/D = 75$

Looking further downstream for the shaped holes, Figure 9 reveals that the reaction still has an impact at 75 hole diameters. The difference between the air and nitrogen injections has diminished at this distance but it is still prevalent causing about a 5 to 10% enhancement with air particularly at the lower blowing ratios. At the higher blowing ratios, little coolant would be expected at this downstream location, so it is not surprising to see little variation. One note is that the overall heat flux is calculated to be higher at this location than at $x/D = 20$. This is attributed to the greater amount of cooling water present downstream pulling more heat out of the test surface. The actual surface temperatures are 30 to 80 K lower at $x/D = 75$ than at $x/D = 20$. Table 2 gives the variation in surface temperature for the fan holes for four different equivalence ratios at a blowing ratio of 1.0. Readily apparent is the larger deltas at the higher Φ .

Table 2. Comparison of Surface Temperatures at Different Equivalence Ratios for $M = 1.0$ for the Shaped Holes

Φ	X	$T_{s,Air}$ (K)	T_{s,N_2} (K)	% Difference
1.7	20D	790.0	767.1	3.0
	75D	730.4	725.4	0.7
1.5	20D	813.6	764.7	6.4
	75D	739.2	717.5	3.0
0.8	20D	720.2	719.5	0.1
	75D	671.7	669.7	0.3
0.6	20D	632.2	631.5	0.1
	75D	597.9	597.4	0.1

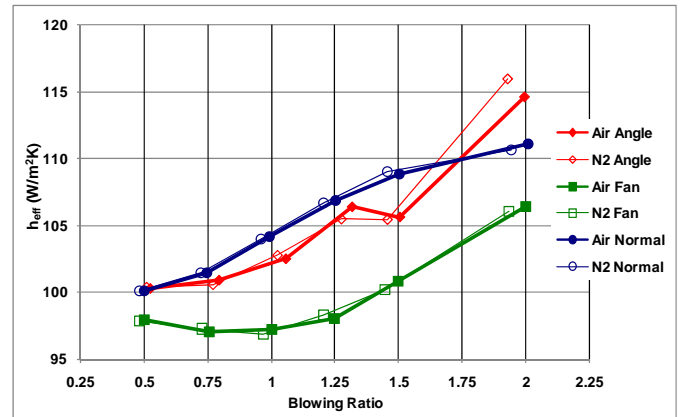


Figure 10. Comparison of cooling hole geometries: Dependence of h_{eff} on M , $\Phi = 0.6$, $x/D = 20$

One means of normalizing the differences of these results for the various cooling configurations was to utilize an effective heat transfer coefficient (h_{eff}). The values of h_{eff} for each of the geometries are compared in Figures 10, 11, and 12. Figure 10 displays h_{eff} for the angled, fan shaped, and normal holes at $\Phi = 0.6$. The data for cooling air (closed symbols) and cooling nitrogen (open symbols) are nearly coincident for the three geometries, indicating that boundary layer reactions had no

effect on h_{eff} at this Φ . Furthermore the basic trends of the data show the angled holes performed better (maintained a lower h_{eff}) than the normal holes at lower M , however performance degrades at higher M due to separation. The fan shaped hole design provided much lower h_{eff} over the entire range of tested values of M .

Figure 11 shows the h_{eff} data for the same cooling geometries at $\Phi = 1.5$. The effect of boundary layer reactions can be clearly observed by comparison of the air and nitrogen data. When air is introduced, a significant increase in effective heat transfer coefficient was experienced for each geometry. The h_{eff} of the normal jets increased by an average of 8% when coolant was switched from nitrogen to air. The h_{eff} for angled holes increased by an average of 14%, while the fan shaped holes increased by 19%. This caused the fan shaped holes, which were the most effective in the nonreactive flow conditions, to be the least effective (highest h_{eff}) for the lower blowing ratios. Interestingly, the shape of the curve changed for the fan shaped holes as well. The previous minimum value of h_{eff} at $M = 1$ has increased by 25% to one of the highest levels of h_{eff} . This reemphasizes that the fan shaped holes which, by design, maintain the film coolant close to the wall, has a negative impact in a reacting flow. Any reactions that occur do so next to the wall for this cooling scheme, resulting in a significant increase in the surface temperature.

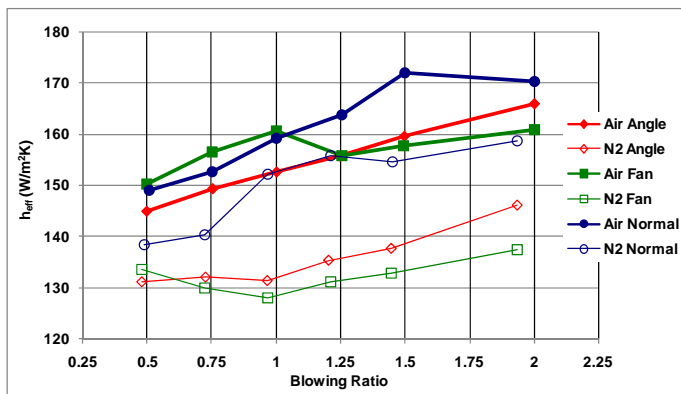


Figure 11. Comparison of cooling hole geometries: Dependence of h_{eff} on M , $\Phi = 1.5$, $x/D = 20$

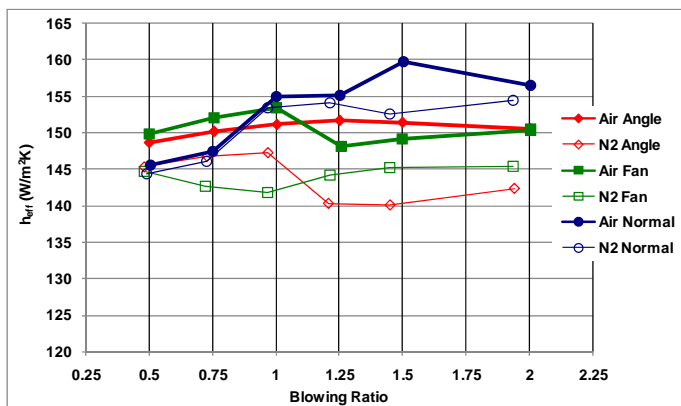


Figure 12. Comparison of cooling hole geometries: Dependence of h_{eff} on M , $\Phi = 1.5$, $x/D = 75$

Looking farther downstream to the 75 D location, Figure 12 provides similar results at the equivalence ratio of 1.5. While the overall levels have been reduced, the same trends are readily apparent which suggests one of two potential drivers. One explanation is that the reaction times are sufficiently long to last an additional 55 hole diameters downstream. In other words the Damkohler number (Da), near 0.68 for this experiment, is such that this reaction was still completing over this surface length. Some simple reaction rate calculations were performed which shows that the carbon and air reaction would require about 1.62 ms to complete in this experiment and that the flow would take about 1.1 ms to traverse from the cooling hole to the downstream set of gauges so it is possible the reaction was still occurring at the downstream location. The second potential driver stems from the belief that the reaction was only occurring on the edge of the coolant jets. The literature has shown (Moore et al. [14] for example) that high vorticity is generated along the interface with the freestream and this mixing zone is where combustion is likely to occur. As the jet progresses downstream, more oxygen was convected out of the core where it could react with the fuel rich freestream. This process continued with downstream distance until the air was depleted from the core. The fact that the normal holes show little enhancement at this downstream position for low blowing ratios further reinforces these drivers. The normal jet ejected the flow further away from the wall leaving less oxygen near the wall at the downstream location.

CONCLUSIONS

This study has focused on the potential for heat release to occur within a turbine as a result of the interaction of air rich cooling flow with the exhaust of a fuel-rich well-stirred-reactor operating at high temperatures over a flat plate. A test rig was designed and constructed with modular components to allow the study of different cooling hole geometries. This investigation focused on three common configurations used in modern turbines – normal holes, angled holes, and fan shaped cooling holes. The cooling holes could be fed with either air or nitrogen, which enabled a direct comparison of the impact of the reactions to be isolated. The heat flux and effective heat transfer coefficient were calculated for a variety of equivalence ratios and blowing ratios for the three cooling hole geometries.

This investigation has shown that reactions do occur downstream of the introduction of cooling film in the presence of a combustor exhaust stream containing unburned fuel. These reactions occurred close to the surface, and resulted in augmented heat transfer to the metal and only happened for equivalence ratios above stoichiometric. The relative impact of the reactions on the surface heat transfer was quantified for the three cooling arrangements. The normal holes resulted in the lowest enhancement of heat transfer to the surface. This was attributed to the high amount of separation resulting in the reactions occurring off the wall surface. The angled holes were more susceptible to reaction as the coolant was introduced along the wall, thus significantly raising the local driving temperature to the wall. The fan shaped holes exhibited the

greatest degradation of performance since the well attached film of coolant that was produced by this design resulted in reactions occurring even closer to that wall and more spread along the wall. This resulted in the highest overall heat load and the greatest difference between the nitrogen injection and the air injection. Overall, the results were consistent with blowing ratio from the perspective of understanding where the jet would be located for the specific case. A turbine cooling scheme designed to take advantage of the improved performance of the fan shaped holes in a nonreactive condition could under-predict the magnitude of augmented heat release due to fuel streaks, potentially resulting in turbine durability degradation.

Further investigations are planned to better understand two main areas of concern. First, an improved quantification of the inlet chemistry in the upstream boundary condition to the film cooling jet is desired. Laser diagnostics will be used to aide in the identification of the species that has a significant impact on the reaction. Second, diagnostic lasers will also be used to help quantify the location of the reaction and, more precisely, the extent of the reaction. Clearly reactions can occur in a configuration such as an Intra Turbine Burner and further investigations are needed to address relevant design issues.

ACKNOWLEDGMENTS

The authors are grateful to Jeff Brown and Lt. Joe Beck of the Air Force Research Lab Structures Branch in the Turbine Engine Division for their model of the temperature distributions within the test block. We are further grateful to Dr. Paul King of the Air Force Institute of Technology for his advice during this project. We also wish to acknowledge Chuck Abel of ISSI and Mike Arstingstall of UDRI for their assistance in machining the test pieces and running the experiments, respectively.

REFERENCES

- [1] Bogard, D.G., and Thole, K.A., "Gas Turbine Film Cooling," *Journal of Propulsion and Power*, Vol. 22, 2006, pp. 249-269.
- [2] Baldauf, S., Schulz, A., and Wittig, S., "High-Resolution Measurements of Local Effectiveness From Discrete Hole Film Cooling," *Journal of Turbomachinery*, Vol. 123, 2001, pp. 758-765.
- [3] Saumweber, C., Schulz, A., and Wittig, S., "Free-Stream Turbulence Effects on Film Cooling with Shaped Holes," *Journal of Turbomachinery*, Vol. 125, 2003, pp. 65-73.
- [4] Mattingly, J.D., Heiser, W.H., Daley, D.H., *Aircraft Engine Design*. Washington DC: AIAA, 1987.
- [5] Zelina, J., Sturgess, G.J., Shouse, D.T., "The Behavior of an Ultra-Compact Combustor (UCC) Based on Centrifugally Enhanced Turbulent Burning Rates," AIAA Paper No. 2004-3541, 2004.
- [6] Zelina, J., Shouse, D. T., and Hancock, R.D., "Ultra-Compact Combustors for Advanced Gas Turbine Engines," 2004-GT-53155, 2004.
- [7] Lukachko, S.P., Kirk, D.R., Waitz, I.A., "Turbine Durability Impacts of High Fuel-Air Ratio Combustors, Part 1: Potential For Intra-Turbine Oxidation of Partially-Reacted Fuel," GT-2002-30077, 2002.
- [8] Kirk, D.R., Guenette, G.R., Lukachko, S.P., and Waitz, I.A., "Gas Turbine Engine Durability Impacts of High Fuel-Air Ratio Combustors Part 2: Near Wall Reaction Effects on Film-Cooled Heat Transfer," GT-2002-30182, 2002.
- [9] Nenniger, J.E., Kridiotis, A., Chomiak, J., Longwell, J. P., and Sarofim, A. F., "Characterization of a Toroidal Well Stirred Reactor," *Twentieth Symposium (International) on Combustion*, The Combustion Institute, pp. 473-479, 1984.
- [10] Zelina, J., "Combustion Studies in a Well-Stirred Reactor," Ph.D. Thesis, University of Dayton, Dayton OH, 1995.
- [11] Stouffer, S.D., Striebich, R.C., Frayne, C. W., and Zelina, J., "Combustion Particulates Mitigation Investigation Using a Well-Stirred Reactor," AIAA Paper No. 2002-3723, 2002.
- [12] Stouffer, S., Pawlik, R., Justinger, G., Heyne, J., Zelina, J., and Ballal, D., "Combustion Performance and Emissions Characteristics for A Well-Stirred Reactor for Low Volatility Hydrocarbon Fuels", AIAA Paper No. 2007-5663, 2007.
- [13] Evans, Dave S., King, Paul I., Polanka Marc D., Zelina, Joseph, Anderson, Wesley S., and Stouffer, Scott D., "The Impact of Heat Release in Turbine Film Cooling" AIAA Paper No. 2009-298.
- [14] Moore, K., Wolff, J.M., Polanka, M.D., and Sondergaard, R., "A Large Scale Investigation of a Flat Plate Vortex Generator Jet in Crossflow using PIV", 41st AIAA/ASME/SAE/ASEE Joint Propulsion Conference and Exhibit, AIAA-2005-4221, Tucson, AZ, 10-13 July 2005.